

Hard-core Bose-Fermi mixture in one-dimensional split traps

Xiaolong Lü,¹ Xiangguo Yin,² and Yunbo Zhang^{1,*}

¹*Institute of Theoretical Physics, Shanxi University, Taiyuan 030006, People's Republic of China*

²*Institute of Physics, Chinese Academy of Sciences, Beijing 100086, People's Republic of China*

(Dated: February 23, 2024)

We consider a strongly interacting one-dimensional (1D) Bose-Fermi mixture confined in a hard wall trap or a harmonic oscillator trap with a tunable δ -function barrier at the trap center. The mixture consists of 1D Bose gas with repulsive interactions and of 1D noninteracting spin-aligned Fermi gas, both species interacting through hard-core interactions. Using a generalized Bose-Fermi mapping, we calculated the reduced single-particle density matrix and the momentum distribution of the gas as a function of barrier strength and the parity of particle number. The secondary peaks in the momentum distribution show remarkable correlation between particles on the two sides of the split.

PACS numbers: 03.75.Mn, 67.85.Pq, 37.10.Gh

I. INTRODUCTION

In recent years the strongly interacting ultra-cold atoms system in quasi-one dimensional(1D) have attracted great interests both in experiments and theories. With two perpendicular optical lattices to realize the 1D system and Feshbach resonance or the confinement-induced resonance to tune the 1D effective interacting strength, Tonks-Girardeau(TG) gas [1, 2], a Bose-Einstein condensate in which the repulsive interactions between bosonic particles dominate the physics of the system, has been realized in experiments. For strong attractive interactions between atoms, the Super Tonks-Girardeau gas [3] represents an excited quantum gas phase in a 1D spatial geometry. Sudden switching from infinitely strong repulsive to infinitely attractive interactions stabilizes the gas against collapse and connects the ground state of the Tonks gas to the excited state of the Super Tonks gas. Meanwhile, the study of a two spin mixture of 1D strongly interacting fermions gas at finite spin imbalance demonstrates how ultracold atomic gases in 1D may be used to create non-trivial new phases of matter experimentally [4, 5]. Despite intense theoretical and experimental efforts, however, the strongly interacting Bose-Fermi mixtures remains largely elusive, where interesting phenomena such as phase separation are predicted to occur [6–9].

Most of the theoretical research on Bose-Fermi mixtures so far has been concentrated on three dimensional systems, and only recently 1D systems started attracting attention. Theoretical investigations on the quasi-1D Bose-Fermi mixture so far have focused on the phase diagrams, ground-state and thermodynamical properties in the scheme of Luttinger liquid theory [10, 11] and Bethe ansatz method [9, 12]. For the 1D ultra-cold atoms system with infinity repulsive interaction between particles, the Fermi-Bose Mapping (FBM) theorem is used to de-

rive the wavefunctions and ground state properties of the system. In the simplest case the mapping function relates the system of impenetrable bosons with that of non-interacting fermions [13] and similar schemes have been extended to various hard-core systems like spinor Bose gases [14], spin-1/2 fermions [15] and Bose-Fermi mixture [16].

The starting point of the many-particle solutions of a given geometry for the TG gas is the exact single-particle eigenstates. Given the limited examples of exactly solvable single-particle problems in quantum mechanics, exactly solvable many-particle problems are also rare even in the TG limit. Here we choose two typical split traps to load the mixture, i.e., a split hard wall and a split harmonic oscillator. Investigating the model of the δ -split potential can be justified in several ways and related works have been done [17–20]. For mesoscopic systems, the ground state properties qualitatively differ for system with a split at the trap center, especially when the number of particles is odd. On the other hand, δ -split potential may be viewed as a generic model for double-well structures or, alternatively, as a good approximation to the problem of a trap with an impurity at the center. Experimentally this kind of split is easy to realize by adding an additional laser in the trap center [21]. Tunneling of particles through an energetically forbidden region reveals more and more experimentally accessible examples of nontrivial quantum phases [22–25].

The paper is organized as follows. After a brief introduction of the many-body system, in Sec. II we review the Fermi-Bose mapping theorem for Bose-Fermi mixture and describe the associated single-particle eigenfunctions and eigenvalues of the δ -split traps. In Sec. III we calculate the reduced single-particle density matrix and investigate the influence of the splitting strength on the momentum distribution which is experimentally accessible. We observe the emergence of bimodal secondary peaks at the neck of the central peaks for various barrier strengths and analyze the parity effect of the total number of atoms. Finally, in Sec. IV we make concluding remarks.

*Electronic address: ybzhang@sxu.edu.cn

II. BOSONS AND FERMIONS IN SPLIT TRAPS

Consider a mixture of N_B bosons and N_F fermions trapped in a tight atomic waveguide which restricts the dynamics of the system into a quasi one-dimensional system in the longitudinal direction. Assume that the interaction potentials are short-ranged, the many-particle Hamiltonian at low linear density can be written as

$$H = \int dx \left\{ \Psi_b^\dagger \left(-\frac{\hbar^2}{2m_b} \partial_x^2 + V_b(x) \right) \Psi_b + \Psi_f^\dagger \left(-\frac{\hbar^2}{2m_f} \partial_x^2 + V_f(x) \right) \Psi_f + \frac{1}{2} g_{bb} \Psi_b^\dagger \Psi_b^\dagger \Psi_b \Psi_b + g_{bf} \Psi_b^\dagger \Psi_b^\dagger \Psi_f \Psi_f \right\}, \quad (1)$$

Here, Ψ_b , Ψ_f are the boson and fermion field operators. The bosonic and fermionic particles are assumed to share the same mass $m_b = m_f = m$, which could be realized by choosing different isotopes of a given alkali element, e.g. ^{40}K - $^{39(41)}\text{K}$ [26] or $^{86(84)}\text{Rb}$ - $^{87(85)}\text{Rb}$ [27]. In our model, the particles experience both boson-boson (g_{bb}) and boson-fermion (g_{bf}) contact interactions, while the fermion-fermion interaction is forbidden by the Pauli exclusive principle ($g_{ff} = 0$). We also assume the trapping potential are exactly the same for both fermions and bosons, $V_b(x) = V_f(x) = V(x)$.

A. The Fermi-Bose mapping

The original Fermi-Bose mapping theorem only related strongly interacting bosons to ideal fermions [13]. It was recently found that the mapping idea can be applied to Fermi Tonks gas and to a series mixture system as well [16]. Concentrating on the situation relevant to our system, we denote the space coordinates by $X = (x_1, x_2, \dots, x_N)$, where x_i is the coordinate of a boson when $i \in \{1, \dots, N_B\}$, or else it labels a fermion provided that $i \in \{N_B + 1, \dots, N_B + N_F = N\}$. Under the hard-core condition $g_{bb}, g_{bf} \rightarrow \infty$, we may safely drop the two interaction energies in the Hamiltonian and as a result the many-body wave function of the system is subject to a constraint that

$$\Phi(X) = 0, \quad \text{if} \quad x_i = x_j \quad (2)$$

for $i \neq j$. The first quantized Hamiltonian of our boson-fermion mixture is then a sum of one-body operators, $H = \sum_{i=1}^N h_i$, where

$$h_i = -\frac{\hbar^2}{2m} \partial_{x_i}^2 + V(x_i). \quad (3)$$

Using the Fermi-Bose mapping theorem [16], the total wave function $\Phi(X)$ satisfying the constraint is constructed as

$$\Phi(X) = A(X) \Phi_D(X), \quad (4)$$

where $\Phi_D(X)$ is a Slater determinant of N orthonormal orbitals $u_1(x), u_2(x), \dots, u_N(x)$ occupied by N particles

$$\Phi_D(X) = \sum_P \varepsilon(P) u_1(Px_1) u_2(Px_2) \dots u_N(Px_N). \quad (5)$$

The sum runs over all $N!$ possible permutations of these variables including permutations exchanging bosons with fermions, and $\varepsilon(P) = \pm 1$ for even/odd times of permutation. The symmetry of the system is repaired by the mapping function $A(X)$

$$A(X) = \prod_{1 \leq j < l \leq N_B} \text{sgn}(x_j - x_l) \prod_{j=1}^{N_B} \prod_{l=N_B+1}^N \text{sgn}(x_j - x_l) \quad (6)$$

so that in general the wavefunction is symmetric under permutations of bosons and antisymmetric under permutation of fermions. The sign function $\text{sgn}(x)$ is $+1(-1)$ for $x > 0(x < 0)$.

B. Eigenstates and eigenvalues of the δ -split traps

The orthonormal orbitals $u_n(x)$ are eigenfunctions of the single-particle Hamiltonian with eigenvalues ϵ_n

$$\left(-\frac{\hbar^2}{2m} \partial_x^2 + V(x) \right) u_n(x) = \epsilon_n u_n(x) \quad (7)$$

with $n = 1, 2, \dots, N$. In this paper we consider the case that the mixture is subjected to two kinds of split external trapping potentials, that is, (A) a hard wall trap which is zero in the region $(-a, a)$ and infinite outside, and (B) a harmonic oscillator potential with frequency ω , both with a δ -type barrier located at the origin $x = 0$. We denote the strength of this barrier by a positive parameter κ . Thus

$$V(x) = \begin{cases} \kappa \delta(x), & |x| < a, \\ \infty, & |x| \geq a. \end{cases} \quad (8)$$

for model (A) and

$$V(x) = \frac{1}{2} m \omega^2 x^2 + \kappa \delta(x) \quad (9)$$

for model (B). The single-particle eigenstates of the delta-split hard wall trap can be found in quantum mechanics textbook, and those of the delta-split harmonic oscillator have recently been discussed in ref [28] and we will briefly review the solutions here for completeness.

The eigenfunctions are either symmetric or antisymmetric due to the parity of both potentials. For model (A), the analytic symmetric eigenfunctions are

$$u_n(x) = C \left(\cos(kx) + \frac{m\kappa}{\hbar^2 k} \sin(k|x|) \right) \quad (10)$$

for $|x| < a$, and $u_n(x) = 0$ for $|x| \geq a$. Here, C is the normalization constant and k is the wave vector of the particle, determined by $\tan(ka) = -\hbar^2 k / m\kappa$. The eigenenergies $E = \hbar^2 k^2 / 2m$ are given by the graphical solutions

of k , that is, the intersection points of the straight line $-\hbar^2 k/m\kappa$ and the tangent function which can be labeled as $n = 1, 3, 5, \dots$. As $\kappa \rightarrow 0$, the eigenenergies reduce to those of the ordinary infinite well of width $2a$. As $\kappa \rightarrow \infty$, the barrier becomes impenetrable, and we have two isolated infinite square wells of width a . By contrast, the antisymmetric eigenfunctions are zero at the origin, so they never “feel” the delta function at all. The eigenfunctions and eigenenergies are exactly the same as those for the infinite square well of width $2a$

$$u_n(x) = C \sin(kx) \quad (11)$$

with $k = n\pi/2a$ and $E_n = n^2\pi^2\hbar^2/2m(2a)^2$ ($n = 2, 4, 6, \dots$). We will use dimensional variables in units of the half split square potential length a , all momenta in units of $p = \hbar/2a$, and all energies in units of $\pi^2\hbar^2/2ma^2$.

For model (B), we immediately know that the antisymmetric eigenfunctions of the simple harmonic oscillator remain good eigenfunctions for the δ -split oscillator, as they vanish at the exact position of the disturbance. We have

$$u_n(x) = N_n H_n(Q) e^{-Q^2/2} \quad (12)$$

where $N_n = (\sqrt{\pi} 2^n n! x_{osc})^{-1/2}$ with $n = 1, 3, 5, \dots$. Here $Q = x/x_{osc}$, $x_{osc} = \sqrt{\hbar/m\omega}$ and $H_n(Q)$ are the n -th order Hermite polynomials. The corresponding energies are given by the eigenvalues of the odd parity states of the harmonic oscillator $E_n = (n + 1/2)\hbar\omega$.

The even eigenstates of the simple harmonic oscillator, on the other hand, have an extremum at $x = 0$. They are therefore strongly influenced by the splitting potential and can be found to be [18, 28]

$$u_n(x) = N_n e^{-Q^2/2} U(-\nu_n, 1/2, Q^2) \quad (13)$$

where $U(a, b, z)$ are the Kummer's confluent hypergeometric functions [29] and $\nu_n \equiv E_n/2\hbar\omega - 1/4$ is the non-integer analog of the principle quantum number n of the harmonic oscillator. The eigenenergies E_n ($n = 0, 2, 4, \dots$) are given by the solution of

$$2\Gamma(-\nu_n + 1/2) + \kappa\Gamma(-\nu_n) = 0 \quad (14)$$

Similarly in the following the variables are rescaled in units of the harmonic-oscillator length x_{osc} , the harmonic-oscillator momentum $p_{osc} = \hbar/x_{osc} = \sqrt{m\hbar\omega}$, the harmonic-oscillator energy $\hbar\omega$.

With these single-particle eigenstates, we are now in a position to build the Slater determinant $\Phi_D(X)$ for a system of noninteracting fermions. The Fermi-Bose mapping theorem then allows us for the calculation of the exact many particle wave function $\Phi(X)$ from the fermionic result.

III. MOMENTUM DISTRIBUTIONS OF THE BOSE-FERMI MIXTURE

The quantum correlations of the 1D quantum gases can be obtained from the reduced single-particle density

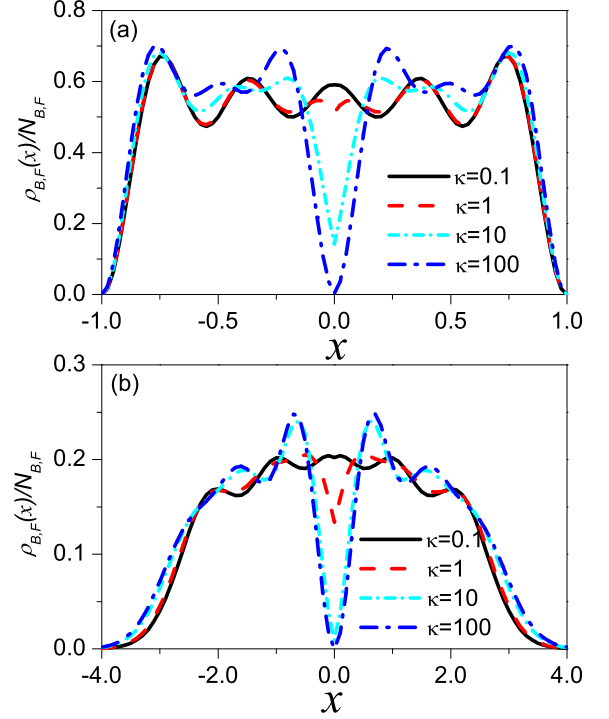


FIG. 1: (Color online) Total density distributions for odd number of atoms ($N = N_B + N_F = 5$) at different strengthes of the split barrier (a) for Model A (x in units of a), (b) for Model B (x in units of $\sqrt{\hbar/m\omega}$).

(RSPD) matrices defined as

$$\begin{aligned} \rho_B(x, y) &= N_B \int dX' \Phi^*(x, X') \Phi^*(y, X') \\ \rho_F(x, y) &= N_F \int dX'' \Phi^*(X'', x) \Phi(X'', y) \end{aligned} \quad (15)$$

for bosons and fermions, respectively. Here $X' = (x_2, \dots, x_N)$ and $X'' = (x_1, \dots, x_{N-1})$. In the TG interaction limit, however, the diagonal elements are nothing but the single-particle density profiles $\rho_B(x, x) = \rho_B(x)$ or $\rho_F(x, x) = \rho_F(x)$ which are exactly the same up to normalization factors due to the fact that the square of the mapping function $A(X)$ in (6) is unity. They both are proportional to the spatial density $\rho_{TG}(x)$ of a trapped TG gas made of N bosons. In Fig 1 we illustrate the normalized density profiles

$$\rho_B(x)/N_B = \rho_F(x)/N_F = \rho_{TG}(x)/N \quad (16)$$

for split hard wall trap (Model A) and split harmonic oscillator (Model B), respectively. Here we are interested in the effect of the δ -barrier in the center and results for four values of the barrier strength $\kappa = 0.1, 1, 10, 100$ are presented. It has been shown that for even number

of particles the barrier separates the particles into two half wells and increasing the barrier strength leads to the emergence of a quadrant separation of which the interference is negligible [8, 20]. Thus only results for odd number of particles are given here and we found that the density profile relies on the total number of particles, instead of the number of bosons and fermions. For negligibly small split barrier, the density profiles present exactly the same number of density maxima as the total number of atoms. The corresponding density profile in the large- N limit is flat in the square well and is a semicircle of radius $R = \sqrt{2N}$ in the harmonic trap. Increasing the barrier strength would gradually cut the density profiles into two symmetric parts and the number of peaks do not match the number of particles any more. This is a clear signature of the coherence inherent in the system, which becomes more pronounced in the momentum distribution. The delta-splitting seems more efficient in suppressing the density in a harmonic oscillator. This can be understood by noticing that the energy unit adopted in hard wall is $\pi^2/2$ times larger than that in harmonic oscillator.

The Fermi-Bose mapping theorem gives identical density distributions of a sample for bosons and fermions in the TG limit. However, the momentum distribution can still be used for distinction, which can be calculated from the reduced single-particle density matrix

$$n_{B,F}(p) = \frac{1}{2\pi} \iint \rho_{B,F}(x, y) e^{-ip(x-y)} dx dy \quad (17)$$

which is normalized to N . The momentum distribution of the bosonic component $n_B(p)$ is equivalent to that of N TG bosons placed within the split traps. This again comes from the fact that the symmetry of both boson-boson and boson-fermion permutations has been repaired in the mapping function and has already been addressed in Ref. [8, 18, 19]. The physical reason for this identical momentum distribution originates from the equal-weighted superposition of the orthonormal orbitals in the construction of the many-body wavefunction (5). Thus we now turn our attention to the behavior of the fermionic momentum distribution in the mixture $n_F(p)$ as a function of the split barrier strengths. The determination of the fermionic momentum distribution proves very complex even in the homogeneous mixture and the extension to the harmonically trapped mixture has been done in Ref. [30]. The calculation is more involved because the expression for the density matrix could not be reduced to a simpler analytical formula, and we have resorted to numerical computations. Following a more convenient scheme, we use the alternative expression for momentum distribution

$$n_F(p) = N \int dX'' \left| \tilde{\Phi}(X'', p) \right|^2 \quad (18)$$

Here $\tilde{\Phi}(X'', p)$ is the Fourier transformation of

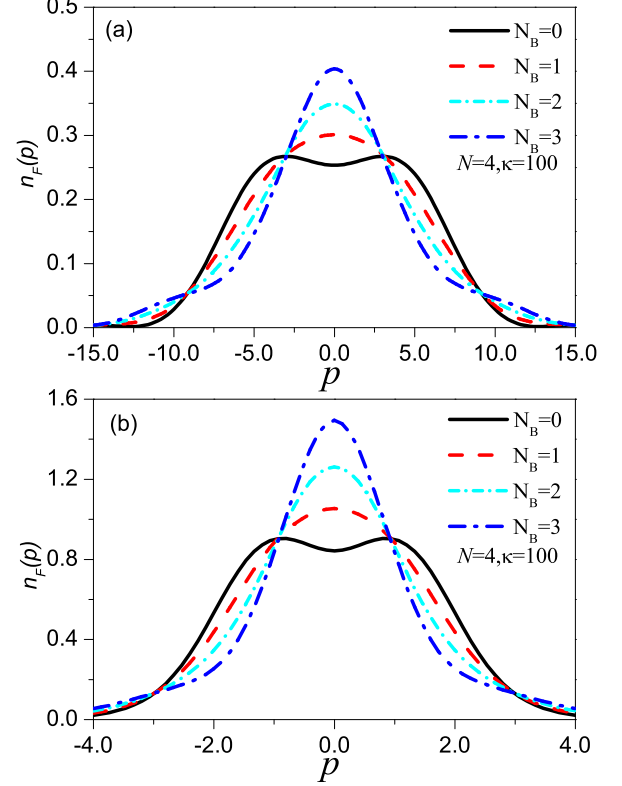


FIG. 2: (Color online) Momentum distributions for even number of atoms ($N = N_B + N_F = 4$) at strong split barrier $\kappa = 100$ (a) for Model A (p in units of $\hbar/2a$), (b) for Model B (p in units of $\sqrt{m\hbar\omega}$).

$\Phi(X'', x_N)$ with respect to the last fermionic variable x_N

$$\tilde{\Phi}(X'', p) = \frac{1}{\sqrt{2\pi}} \int_{-\infty}^{+\infty} dx_N \Phi(X'', x_N) e^{-ipx_N}. \quad (19)$$

In a recent paper, Lelas et al. studied the RSPDM, momentum distribution, natural orbitals and their occupancies for a Bose-Fermi mixture in an alternative form of a harmonic potential with a Gaussian-type barrier in the center, however, for a rather strong fixed barrier, i.e. the barrier is at least several times larger than the energy of the N -th single-particle state of the potential. We present here the results for various barrier strengths and analyze the dependence of the distribution profiles on the parity of the total number of particles. Furthermore our results provide a direct comparison of the momentum distribution for different type of trapping potentials (hard-wall and harmonic oscillator).

Figure 2 shows our results for a mixture with a fixed even total number of $N = 4$ particles when the number of bosons is increased from $N_B = 0$ up to 3. A mixture with $N_B = N$ or $N - 1$ makes no difference because one can not imprint any statistical property onto the only left

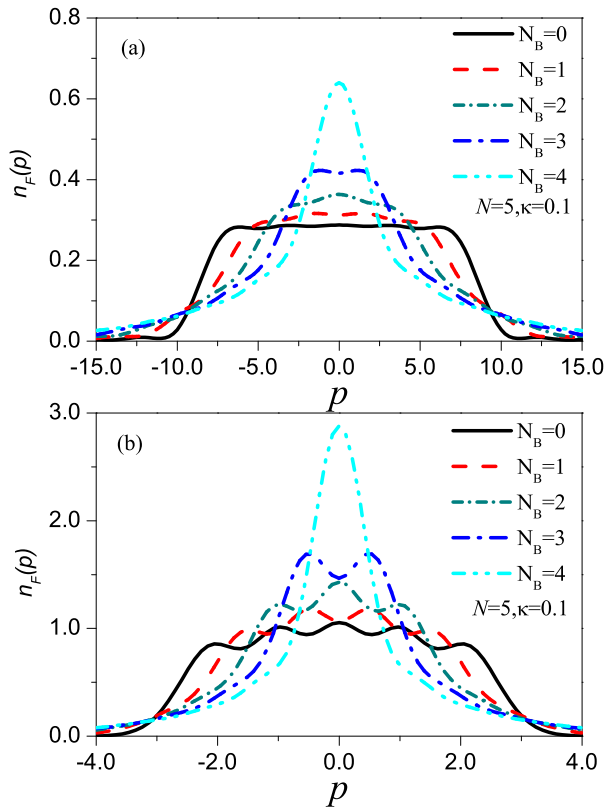


FIG. 3: (Color online) Momentum distributions for odd number of atoms ($N = N_B + N_F = 5$) at weak split barrier $\kappa = 0.1$ (a) for Model A (p in units of $\hbar/2a$), (b) for Model B (p in units of $\sqrt{m\hbar\omega}$).

atom. Both distributions for split hard wall and split harmonic oscillator take smooth bell-shaped profiles, with explicit difference being the characteristic momentum up to which the fermionic momentum distribution is significantly different from zero. The signature of fermionization becomes more evident for less bosons. We also note that the split barrier in the center hardly affect the momentum distribution of even number of atoms, except a little broadening of the momentum distribution and lowering of its peak.

Things become much more different for odd number of particles. We first illustrate the situation for a weak barrier. Figure 3 shows our results for a BF mixture with a fixed total number of $N = 5$ particles when the number of bosons is increased from $N_B = 0$ up to 4 (or, equivalently, 5). We observe N_F “fermionic” oscillations developed in the momentum distribution, yet the oscillations in harmonic oscillator are more prominent. Fermionic oscillations are suppressed for more bosons and the tails of the distribution become more easily seen. Finally, when the atoms in the mixture are all bosons, we see typical Tonks-Girardeau-type momentum distribution.

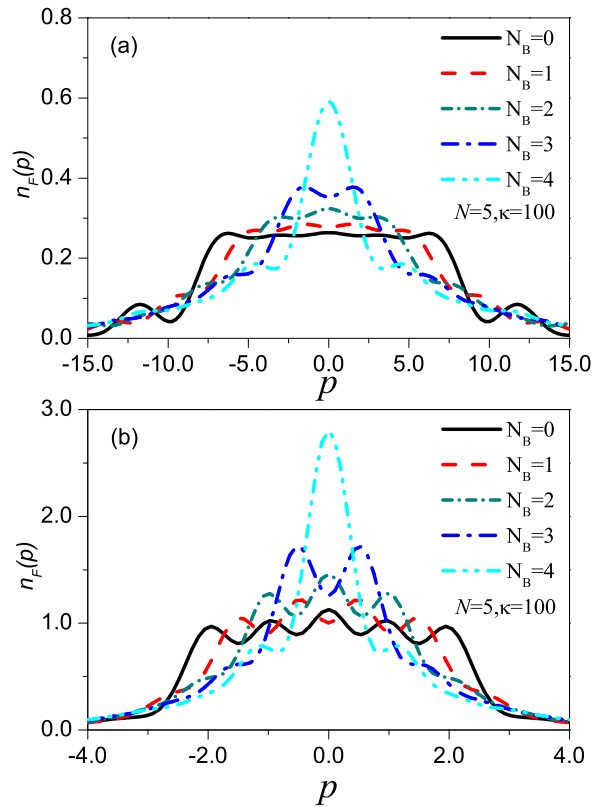


FIG. 4: (Color online) Momentum distributions for odd number of atoms ($N = N_B + N_F = 5$) at strong split barrier $\kappa = 100$ (a) for Model A (p in units of $\hbar/2a$), (b) for Model B (p in units of $\sqrt{m\hbar\omega}$).

A strong split barrier greatly modifies the momentum distribution of odd number of atoms. Quite similar to the bosonic case, one can see the emergence of bimodal secondary peaks at the neck of the central peaks in Figure 4, which stems from the interference of the particles in two almost separate wells. The secondary peaks remain prominent for all combination of bosons and fermions, moving inward when the number of bosons is increased. Again we observe that the characteristic momentum is notably different for the square well and for the harmonic confinement. For the square well it is of the order of $k \sim \pi N/2$, while for the harmonic trap it goes as $k \sim \sqrt{2N}$. The large- N asymptotic in absence of bosons in both cases is step function.

IV. CONCLUSION

In conclusion, we have shown the ground state properties of a Bose-Fermi mixture in split potential wells. We observe that the most significant difference between the total even and odd numbers of particles occurs in the

emergence of bimodal secondary peaks in the momentum distributions. Three critical features can be seen (1) the momentum distribution depends on the ratio of the bosons and fermions in the mixture, as well as the total number of the atoms; (2) the presence of a strong split barrier at the trap center enhance greatly the correlation of the atoms on the two separated wells; (3) the dependence of characteristic momentum on the number of atoms relies on the shape of trapping potential.

Acknowledgments

This work is supported by NSF of China under Grant No. 10774095, NSF of Shanxi Province under grant No. 2009011002, National Basic Research Program of China (973 Program) under Grant Nos. 2006CB921102 and 2010CB923103, and Program for New Century Excellent Talents in University (NCET).

-
- [1] B. Paredes, A. Widera, V. Murg, O. Mandel, S. Fölling, I. Cirac, G. V. Shlyapnikov, T. W. Hänsch, and I. Bloch, *Nature* **429**, 277 (2004).
 - [2] T. Kinoshita, T. Wenger, and D. S. Weiss, *Science* **305**, 1125 (2004).
 - [3] E. Haller, M. Gustavsson, M. J. Mark, J. G. Danzl, G. Hart, G. Pupillo, and H.-C. Nägerl, *Science* **325**, 1224 (2009).
 - [4] H. Moritz, T. Stöferle, K. Günter, M. Köhl, and T. Esslinger, *Phys. Rev. Lett.* **94**, 210401 (2005).
 - [5] Y. Liao, A. S. C. Rittner, T. Paprotta, W. Li, G. B. Partridge, R. G. Hulet, S. K. Baur, and E. J. Mueller, *arXiv:0912.0092*.
 - [6] C. K. Lai, C. N. Yang, *Phys. Rev. A* **3**, 393 (1971); C. K. Lai, *J. Math. Phys.* **15**, 954 (1974).
 - [7] K. K. Das, *Phys. Rev. Lett.* **90**, 170403(2003).
 - [8] X. Yin, S. Chen, and Y. Zhang, *Phys. Rev. A* **79**, 053604 (2009).
 - [9] A. Imambekov, E. Demler, *Ann. Phys. (N.Y.)* **321**, 2390 (2006); *Phys. Rev. A* **73**, 021602(R) (2006).
 - [10] M. A. Cazalilla, A. F. Ho, *Phys. Rev. Lett.* **91**, 150403 (2003).
 - [11] L. Mathey, D. W. Wang, W. Hofstetter, M. D. Lukin, and E. Demler, *Phys. Rev. Lett.* **93**, 120404 (2004).
 - [12] M. T. Batchelor, M. Bortz, X.-W. Guan, and N. Oelkers, *Phys. Rev. A* **72**, 061603(R) (2005); X.-W. Guan, M. T. Batchelor, and J.-Y. Lee, *ibid.* **78**, 023621 (2008).
 - [13] M. Girardeau, *J. Math. Phys. (N.Y.)* **1**, 516 (1960).
 - [14] F. Deuretzbacher, K. Fredenhagen, D. Becker, K. Bongs, K. Sengstock, and D. Pfannkuche, *Phys. Rev. Lett.* **100**, 160405 (2008).
 - [15] L. Guan, S. Chen, Y. Wang, and Z.-Q. Ma, *Phys. Rev. Lett.* **102**, 160402 (2009).
 - [16] M. D. Girardeau and A. Minguzzi, *Phys. Rev. Lett.* **99**, 230402 (2007).
 - [17] X. Yin, Y. Hao, S. Chen, and Y. Zhang, *Phys. Rev. A* **78**, 013604 (2008).
 - [18] J. Goold and Th. Busch, *Phys. Rev. A* **77**, 063601 (2008).
 - [19] K. Lelas, D. Jukić and H. Buljan, *Phys. Rev. A* **80**, 053617 (2009).
 - [20] D. S. Murphy, J. F. McCann, J. Goold, and T. Busch, *Phys. Rev. A* **76**, 053616 (2007).
 - [21] T. P. Meyrath, F. Schreck, J. L. Hanssen, C.-S. Chuu, and M. G. Raizen, *Phys. Rev. A* **71**, 041604(R) (2005).
 - [22] X. Cai, L. Guan, S. Chen, Y. Hao, and Y. Wang, *arXiv:0909.5523*.
 - [23] A. C. Pflanzner, S. Zöllner, P. Schmelcher, *arXiv:0911.5142*.
 - [24] S. Zöllner, H.-D. Meyer, and P. Schmelcher, *Phys. Rev. Lett.* **100**, 040401 (2008); *Phys. Rev. A* **78**, 013629 (2008); **74**, 053612 (2006).
 - [25] Y. Hao, Y. Zhang, J.-Q. Liang, and S. Chen, *Phys. Rev. A* **73**, 063617 (2006).
 - [26] R. Côté, A. Dalgarno, H. Wang and W. C. Stwalley, *Phys. Rev. A* **57**, R4118 (1998).
 - [27] J. P. Burke, J. L. Bohn, *Phys. Rev. A* **59**, 1303 (1999); S. G. Crane, X. Zhao, W. Taylor and D. J. Vieira, *Phys. Rev. A* **62**, 011402(R) (2000).
 - [28] Th. Busch, B. G. Englert, K. Rzazewski, and M. Wilkens, *Found. Phys.* **28**, 549 (1998).
 - [29] M. Abramowitz and I. A. Stegun, eds., *Handbook of Mathematical Functions* (Dover, New York, 1972).
 - [30] B. Fang, P. Vignolo, C. Miniatura and A. Minguzzi, *Phys. Rev. A* **79**, 023623 (2009).